Reactive Ligand Influence on Initiation in Phenylene Catalyst-Transfer Polymerization

Ariana O. Hall,[1] Se Ryeon Lee,[1] Andrea N. Bootsma,[2] Jacob W. G. Bloom,[2] Steven E. Wheeler,[2] Anne J. McNeil[1]

[1]Department of Chemistry and Macromolecular Science and Engineering Program, University of Michigan, 930 North University Avenue, Ann Arbor, Michigan 48109-1055
[2]Department of Chemistry, Texas A&M University, PO Box 30012, College Station, Texas 77842–3012
Correspondence to: A. J. McNeil (E-mail: ajmcneil@umich.edu)

ABSTRACT: Synthesizing conjugated polymers via catalyst-transfer polymerization (CTP) has led to unprecedented control over polymer sequence and molecular weight. Yet many challenges remain, including broadening the monomer scope and narrowing the molecular weight dispersities. Broad polymer dispersities can arise from nonliving pathways as well as slow initiation. Previously, slow initiation was observed in Ni-mediated CTP of phenylene monomers. Although precatalysts with faster initiation rates have been reported, the rates still do not exceed propagation. Herein a second- and third-generation of reactive ligands are described, along with a simple method for measuring initiation rates. A precatalyst with an initiation rate that exceeds propagation is now reported, however, the resulting polymer samples still exhibit broad dispersities, suggesting that slow initiation is not the most significant contributing factor in Ni-mediated phenylene polymerizations. In addition, initiation rates measured under authentic polymerization conditions revealed that both exogenous triphenylphosphine and an *ortho*-trifluoroethoxy substituent on the reactive ligand have a strong influence. © 2017 Wiley Periodicals, Inc. J. Polym. Sci., Part A: Polym. Chem. 2017, 55, 1530–1535

KEYWORDS: catalysis; chain-growth polymerization; conjugated polymer; initiation; Ni

INTRODUCTION Catalyst-transfer polymerization (CTP) is a chain-growth method for synthesizing π-conjugated polymers with control over both the polymer length and sequence.[1,2] Though limited in scope, these methods have substantially impacted the field by enabling unprecedented access to materials such as gradient sequence copolymers[3] and a cyclic polymer.[4] Nevertheless, many challenges remain, including broadening the scope to include electron-deficient monomers, narrowing the polymer dispersities, and reducing the air- and moisture-sensitivities of the reagents. Broad dispersities in a chain-growth polymerization reflect underlying problems, including chain-transfer and chain-termination pathways, as well as slow initiation.

Conventional CTP catalyst design has largely focused on the ancillary ligand and metal identity.[2a] In contrast, the mechanistic impact of reactive ligands has remained largely unexplored.[5] Most studies focus on altering the reactive ligand for other purposes, such as growing polymers off surfaces[6] and synthesizing block[7] or cyclic polymers.[4] We recently demonstrated that reactive ligands substantially impact the precatalyst initiation rate in phenylene CTP (Scheme 1).[5] For example, the initiation rate was 132-fold faster with a *para*-dimethylaminobenzene as the reactive ligand compared to the otherwise analogous *para*-fluorobenzene. To rationalize these results, the initiation rates were evaluated computationally, wherein a correlation between the activation barrier for reductive elimination was found with the change in charge on the reactive ligands (as computed by Natural Population Analysis) en route to the rate-limiting transition state. Although the theoretical model identified potential reactive ligands with higher reactivity, their functional groups were incompatible with the Grignard-based polymerization (e.g., NO_2). As a consequence, we describe herein a second and third generation of reactive ligands and their initiation rates. At the same time, we report an improved method for measuring initiation rates using *in situ* infrared (IR) spectroscopy.

Herein, we describe how this combined theoretical/experimental approach led to a new, fast-initiating precatalyst for CTP of monomer **1**. We anticipated that this precatalyst

Additional Supporting Information may be found in the online version of this article.
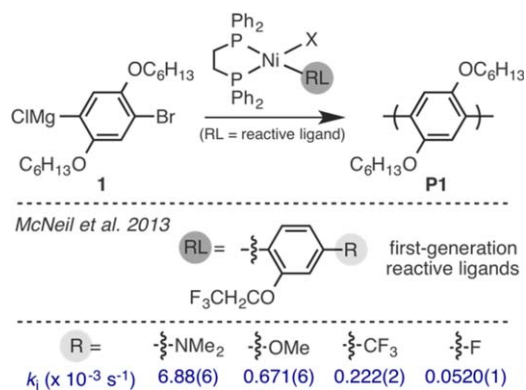
SCHEME 1 First-generation reactive ligands for phenylene polymerization.[5,8] [Color figure can be viewed at wileyonlinelibrary.com]

would lead to polymer samples with narrower dispersities (Đ) because most polymer chains would initiate before any significant propagation occurred. Instead, the dispersities were on par with commonly utilized precatalysts (e.g., (dppe)NiCl$_2$ where dppe is 1,2-bis(diphenylphosphino)-ethane).[9] End-group analysis revealed similar ratios of living/non-living chains, which suggests that other factors (e.g., chain-transfer) are currently more significant contributors to the dispersity. Last, we found that small differences between the original model system and the authentic polymerization conditions led to significantly different initiation rates. Combined, these studies provide useful insight into the effect of reactive ligands on initiation, many of which should be generalizable to CTP of other monomers.

EXPERIMENTAL

Synthesis of Precatalyst 2f

In the glovebox, Ni(cod)$_2$ (138 mg, 0.502 mmol, 1.0 equiv.), and triphenyl phosphine (Ph$_3$P) (262 mg, 1.00 mmol, 2.0 equiv.) were dissolved in THF (3 mL) in a 20 mL vial with stirring. In a separate 4 mL vial, 1-chloro-2-methoxy-4-phenyl-benzene (142 mg, 0.650 mmol, 1.3 equiv.) was dissolved in THF (2 mL). This solution was then added to the vial containing the Ni/Ph$_3$P and stirred at RT for 4 h, during which time a yellow precipitate formed. The solvent was removed under vacuum until approximately 0.5 mL remained. Hexanes (approximately 15 mL) were then added, and the yellow precipitate was collected by vacuum filtration, giving 157 mg (79% yield). In a 20 mL vial, the isolated yellow powder (157 mg, 0.196 mmol, 1.0 equiv.) and 1,2-bis(diphenylphosphino)ethane (94 mg, 0.24 mmol, 1.2 equiv.) were dissolved in THF (2.5 mL) and stirred at RT for 1 h. (Note: A yellow precipitate was observed after 5 min.) After 1 h, hexanes (approximately 15 mL) were added, and the solution was placed in a −30 °C freezer overnight. The product was collected by vacuum filtration, giving 100 mg of **2f** as a yellow powder (59% yield). ^{1}H NMR (500 MHz, CD$_2$Cl$_2$) δ 8.41 (br, 2H) 8.27 (at, J = 9.0 Hz, 2H), 7.71 (at, J = 8.5 Hz, 2H), 7.61–7.40 (m, 11H), 7.34 (at, J = 7.5 Hz, 2H), 7.27–7.22 (m, 2H), 7.17 (at, J = 7.0 Hz, 2H), 7.07 (at, J = 6.6, 2H) 6.85

(at, J = 9.1 Hz, 2H), 6.77 (dt, J = 6.1 Hz, 1.5 Hz, 1H), 6.15 (at, J = 2.1 Hz, 1H), 3.37 (s, 3H), 2.39–2.21 (m, 3H), 1.63–1.62 (m, 1H). ^{31}P NMR (202 MHz, CD$_2$Cl$_2$) δ 59.85 (d, J = 27.5 Hz), 38.37 (d, J = 27.5 Hz).

Representative Procedure for Generating Monomer 1

In a glovebox, a 20 mL vial was charged with 1,4-dibromo-2,6-bishexyloxybenzene (1.09 g, 2.50 mmol, 1 equiv.) and THF (2.5 mL). Then, isopropylmagnesium chloride (1.7 M in THF, 1.32 mL, 2.25 mmol, 0.9 equiv.)[10] was added and the solution stirred at RT for 19 h. The concentration of **1** was determined by titration with salicylaldehyde phenylhydrazone.[11]

General Procedure for Polymerizations Monitored Via In Situ IR Spectroscopy

The IR probe was inserted through an O-ring-sealed 14/20 ground-glass adapter (custom-made) into an oven-dried 50 mL two-neck flask equipped with a stir bar. The other neck was fitted with a three-way flow-control adapter with a septum for injections/aliquot sampling and an N$_2$ line. The oven-dried flask was cooled under vacuum, then filled with N$_2$. The flask was re-evacuated and filled for two additional cycles. The flask was charged with THF (6.7 mL) and cooled to 0 °C for 15 min. After recording a background spectrum, monomer **1** (2.3 mL, 0.44 M in THF, 1.0 equiv.) was added by syringe and equilibrated at 0 °C for at least 5 min. Then the precatalyst solution (1.0 mL, 0.015 M, 0.015 equiv.) was injected and spectra were recorded every 15 s. To account for mixing and temperature equilibration, spectra recorded in the first 60 s were not analyzed.

Aliquots (approximately 0.5 mL) were taken via syringe and immediately quenched with aq. HCl (approximately 1 mL, 12 M). The resulting solution was then extracted with CH$_2$Cl$_2$ (2 × 1.5 mL) (with mild heating if polymer had precipitated), dried over MgSO$_4$, filtered, and then concentrated. At approximately 80% conversion, the polymerization was poured into aq. HCl (20 mL, 12 M), extracted with CH$_2$Cl$_2$ (3 × 25 mL), washed with H$_2$O (1 × 25 mL), brine (1 × 25 mL), dried over MgSO$_4$, filtered, and concentrated. The samples (both aliquots and the final reaction mixture) were each dissolved in THF (with heating), and passed through a 0.2 μm poly(tetrafluoroethylene) filter for analysis by gel permeation chromatography (GPC). The monomer concentration versus time data was calculated from the IR spectra using a calibration curve.

General Procedure for Polymerizations Analyzed by MALDI-TOF-MS

In a glovebox, a precatalyst stock solution was made by combining **2f** (11.2 mg, 0.0165 mmol) with THF (3.3 mL) in a 4 mL vial. (Note: For Ni(dppe)Cl$_2$, a pre-initiation protocol was followed wherein monomer **1** (0.23 mL, 5 equiv.) was added to the precatalyst and stirred until homogeneous.) The precatalyst solution (3.0 mL, 0.015 mmol, 1 equiv.) and THF (3.8 mL) were combined in a 50 mL Schlenk tube, sealed with a Teflon stopper, and then removed from the glovebox and put under N$_2$ pressure. The solution was cooled to 0 °C for 20 min. Then monomer solution (3.2 mL,
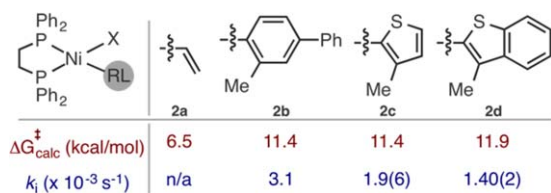
CHART 1 Second-generation reactive ligands.[18] [Color figure can be viewed at wileyonlinelibrary.com]

1.0 mmol, 66 equiv.) was added. After 30 min, an aliquot was removed by syringe, then quenched with aq. HCl (approximately 1.0 mL, 12 M), extracted with CH_2Cl_2 (2 × 1 mL), dried over $MgSO_4$, filtered, concentrated, and then analyzed by MALDI-TOF MS analysis (SI). After 4 h, the polymerization was poured in aq. HCl (20 mL, 12 M), extracted with CH_2Cl_2 (3 × 25 mL), washed with water (1 × 25 mL), brine (1 × 25 mL), dried over $MgSO_4$, filtered, and concentrated. Both the aliquot and the bulk polymerization were analyzed by GPC.

Computational Methods

Computations were performed with the BP86 DFT functional[12] paired with the 6-311+G(d) basis set[13] for all nonmetal atoms and the SDB-cc-pVTZ basis set with the small core, fully relativistic effective core potential[14] for Ni. All computations were performed using Gaussian09.

RESULTS AND DISCUSSION

Influence of Reactive Ligand Structure on Activation Barriers and Rates

We focused on reactive ligands with a carbon-metal bond (Chart 1) because C–C reductive eliminations (i.e., the rate-limiting step) are reported to be faster than the analogous C–Y (where Y = N, O, and S) reductive eliminations.[15] In addition, we focused on sp^2–sp^2 reductive eliminations because they are known to be faster than both sp^2–sp and sp^2–sp^3 reductive eliminations.[16] Our theoretical model predicted that alkenyl reactive ligands (e.g., 2a) would exhibit the lowest barrier (and thus fastest rates) for reductive elimination (Supporting information). Unfortunately, alkenyl-substituted precatalysts decomposed during synthesis, presumably via disproportionation (SI).[17] A biphenyl-based reactive ligand (2b) was prepared based on the rationale that its structural similarity to the polymer would lead to an initiation rate that is similar to propagation. In addition, heteroaryl groups were investigated, including thiophene (2c) and benzothiophene (2d).

In situ IR spectroscopy was used to measure initiation rates under authentic polymerization conditions using monomer 1 (Fig. 1A). When precatalyst initiation is slower than propagation, the initiation rate constant (k_i) can be extracted from the overall rate constant (k_{obs}) at low monomer conversions (i.e., 0–10%, equations 1 and SI).[19] This analysis requires accurately measuring the propagation rate constant (k_p), which can be obtained by monitoring monomer consumption
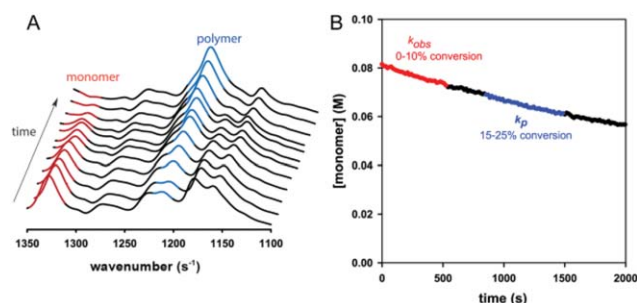

FIGURE 1 (A) Time-dependent *in situ* IR spectra when polymerizing monomer 1 (0.08 M) with precatalyst 2f (0.015 M) in THF at 0 °C. (B) Plot of monomer concentration versus time for the same reaction. [Color figure can be viewed at wileyonlinelibrary.com]

rates at later conversions (e.g., 15–25% conversion) or in a separate experiment (Figs. 1B and SI). Precatalysts 2b–d exhibited initiation rate constants (k_i) on par with our previous best precatalyst (c.f., Scheme 1).[5] On the basis of these studies, it appeared that the potentially more reactive precatalysts (e.g., 2a) are too unstable to isolate while the more stable precatalysts (2b–d) cannot initiate faster than propagation ($k_p = 10(2) × 10^{-3}$/s).

$$k_{obs} = k_i(e^{-k_i t}) + k_p(1 - e^{-k_i t}) \qquad (1)$$

Comparing Initiation Rates under Authentic Conditions Versus the Model System

With the ability to measure initiation rates under the authentic polymerization conditions using *in situ* IR spectroscopy, the question arose as to whether the original model system (which used ^{19}F NMR spectroscopy) measured the true initiation rates. Second-generation precatalyst 2b was used as the test case, and it was modified and evaluated in the same manner as the first-generation reactive ligands.[5] As highlighted in Scheme 2, there were three substantial changes made to the authentic system. First, the bromine atom on the monomer was replaced with a chlorine atom, effectively preventing a second catalyst turnover. Isolating just this modification, a 2.5× slower initiation rate was observed.[20] This modest rate difference reflects the minor
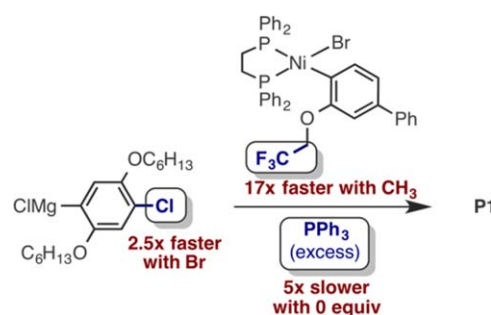
SCHEME 2 Structural differences between the model system (in blue) and the authentic polymerization and their impact on initiation rates (in red). [Color figure can be viewed at wileyonlinelibrary.com]

CHART 2 Third-generation reactive ligands.[18] [Color figure can be viewed at wileyonlinelibrary.com]

impact of switching a Cl to a Br on the monomer's charge density during the reductive elimination.

Next, the influence of Ph$_3$P was examined, which was added in the model system to scavenge Ni(0) generated from the first turnover. These studies revealed a surprising 5× initiation rate enhancement with added Ph$_3$P.[21] One possible explanation is that a five-coordinate square pyramidal species is generated via Ph$_3$P coordination prior to or during reductive elimination.[22] Five-coordinate metal complexes are known to undergo faster reductive eliminations than their four-coordinate counterparts.[10] Related intermediates have been invoked to explain the accelerating effect of added arenes[23] and alkenes[24] on Ni(II)- and Pd(II)-based reductive eliminations. Overall, this Ph$_3$P-based rate acceleration has broader implications for CTP: For example, it may already be accelerating initiation with precatalysts that are generated *in situ* from Ph$_3$P-based precursors (e.g., (PPh$_3$)$_2$NiX$_2$ followed by ancillary ligand exchange).[25] Alternatively, adding exogenous Ph$_3$P may be a simple method to accelerate initiation.[21]

The final difference was the *ortho*-trifluoroethoxy (CF$_3$CH$_2$O) substituent, which was added to provide an NMR spectroscopic handle. The relatively short CH$_2$O linker between the CF$_3$ tag and the reactive arene was a compromise between minimizing the electronic perturbation of the fluorine on reductive elimination while maximizing the likelihood of observing unique ^{19}F signals for each intermediate in the NMR spectrum. The initiation rates with precatalyst **2e** were >17× slower than precatalyst **2f**, suggesting that the fluorine-based inductive effect on reductive elimination is significant (Chart 2). Indeed, our computational model found a lower activation barrier when the CF$_3$ was removed. Such a large inductive effect is reasonable considering the significant difference in pK_a values for CF$_3$CH$_2$OH (12.5) versus CH$_3$OH (15.5).[26]

Combined, these studies provide a cautionary tale about model systems: that is, they can become "talking lions,"[27] which report only on the model system and do not reflect the authentic system.[28] In many cases, including the one described herein, it is only when new methods become available that one can probe the differences between model and authentic systems.

Slow Initiation Is Just One Contributor to Broad Dispersities

When comparing the model system versus authentic conditions, we serendipitously discovered that precatalyst **2f** has the fastest initiation rate measured to date. Our

computational model supported this experimental result, wherein the precatalyst **2f** exhibited a 1 kcal/mol lower activation barrier than precatalyst **2b**. This result is consistent with our earlier observations[5] that resonance-based substituents lead to smaller changes in charge on the reactive ligands during reductive elimination, leading to lower activation barriers and faster rates.

Once this fast initiating precatalyst was identified, we anticipated that the resulting polymer samples would exhibit the narrowest dispersities reported for polymer **P1**. Instead, the dispersities for soluble precatalyst **2f** (Đ = 1.45) were on par with another soluble precatalyst that is widely used ((dppe)Ni(*o*-tolyl)Br, Đ = 1.54) and commercially available insoluble precatalyst (dppe)NiCl$_2$ (Đ = 1.41). Importantly, these polymerization results were obtained using the same monomer batch on the same day and were reproducible. The resulting polymers were analyzed by matrix-assisted laser-desorption ionization time-of-flight mass spectrometry (MALDI-TOF-MS) to identify the polymer end-groups (Fig. 2).[29] Regardless of which precatalyst was used,[30] the majority of polymer chains exhibited end-groups consistent with a living, chain-growth polymerization. The other polymer chains had undergone unproductive pathways such as early termination or chain-transfer. Combined, these results suggest that the ancillary ligand—dppe—needs to be replaced to achieve lower dispersities. Previous studies suggest that a more electron-rich analogue, such as 1,2-bis(diethylphosphino)ethane (depe), would be better due to its stronger metal-polymer associative complex and/or increased reactivity in the subsequent oxidative addition. In practice, however, these air-unstable Ni precatalysts are more difficult to prepare because their synthesis requires transmetalation with (depe)NiCl$_2$ (rather than ligand exchange from
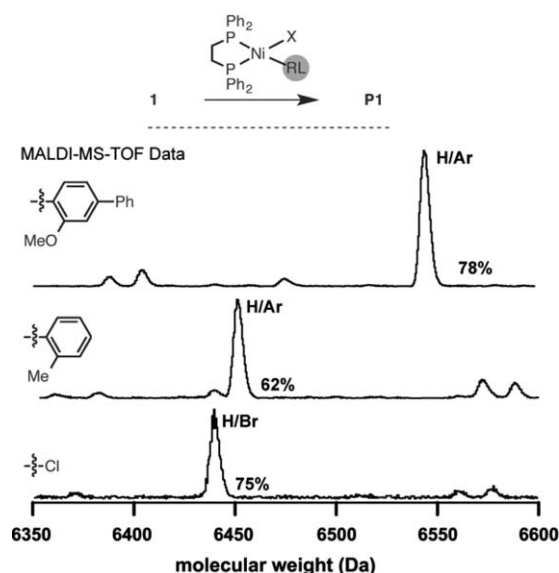

FIGURE 2 MALDI-TOF-MS data when polymerizing monomer **1** (0.10 M) with various (dppe)Ni(RL)X catalysts (1.5 mM; RL is shown) in THF at 0 °C. The major peak corresponds to polymer **P1** with 23 repeat units.

(PPh₃)₂NiArBr), leading to challenging purifications to remove both unreacted starting material and multiple by-products.

CONCLUSIONS

Using a combined theoretical and experimental approach, as well as a new method for measuring initiation, a precatalyst with an initiation rate comparable to propagation was discovered. This faster initiating precatalyst contains a reactive ligand (o-methoxybiphenyl) that closely resembles the polymer structure. These results suggests that more broadly, one may be able to engineer a faster initiating precatalyst by simply focusing on a reactive ligand that is structurally similar to the polymer. Unexpectedly, the polymer dispersities remained quite broad, suggesting that chain-transfer events (e.g., catalyst dissociation) may be prevalent in these polymerizations. This conclusion is supported by the observed 20% of polymer chains that were nonliving. These unproductive events obscured the impact of slow initiation on the dispersities. Nevertheless, we anticipate that these fast-initiating precatalysts will lead to narrower polymer dispersities in phenylene polymerization when alternative ancillary ligands that provide living conditions are used.

ACKNOWLEDGMENTS

REFERENCES

1 (a) E. E. Sheina, J. Liu, M. C. Iovu, D. W. Laird, R. D. McCullough, *Macromolecules* **2004**, *37*, 3526–3528; (b) A. Yokoyama, R. Miyakoshi, T. Yokozawa, *Macromolecules* **2004**, *37*, 1169–1171; (c) R. Miyakoshi, A. Yokoyama, T. Yokozawa, *Macromol. Rapid Commun.* **2004**, *25*, 1663–1666.

2 (a) A. K. Leone, A. J. McNeil, *Acc. Chem. Res.* **2016**, *49*, 2822–2831; (b) T. Yokozawa, Y. Ohta, *Chem. Rev.* **2016**, *116*, 1950–1968; (c) R. Grisorio, G. P. Suranna, *Polym. Chem.* **2015**, *6*, 7781–7795; (d) Z. J. Bryan, A. J. McNeil, *Macromolecules* **2013**, *46*, 8395–8405.

3 (a) T. Hardeman, G. Koeckelberghs, *Macromolecules* **2015**, *48*, 6987–6993; (b) J. A. Amonoo, A. Li, G. E. Purdum, M. E. Sykes, B. Huang, E. F. Palermo, A. J. McNeil, M. Shtein, Y.-L. Loo, P. F. Green, *J. Mater. Chem. A* **2015**, *3*, 20174–20184; (c) E. F. Palermo, S. B. Darling, A. J. McNeil, *J. Mater. Chem. C* **2014**, *2*, 3401–3406; (d) E. F. Palermo, H. L. van der Laan, A. J. McNeil, *Polym. Chem.* **2013**, *4*, 4606–4611.

4 G. R. McKeown, Y. Fang, N. K. Obhi, J. G. Manion, D. F. Perepichka, D. S. Seferos. *ACS Macro Lett.* **2016**, *5*, 1075–1079.

5 S. R. Lee, J. W. G. Bloom, S. E. Wheeler, A. J. McNeil. *Dalton Trans.* **2013**, *42*, 4218–4222.

6 N. E. Huddleston, A. Roy, J. A. Bilbrey, Y. Zhao, J. Locklin, *Macromol. Symp.* **2015**, *351*, 27–36.

7 (a) A. Smeets, P. Willot, J. De Winter, P. Gerbaux, T. Verbiest, G. Koeckelberghs, *Macromolecules* **2011**, *44*, 6017–6025; (b) E. Kaul, V. Senkovskyy, R. Tkachov, V. Bocharova, H. Komber, M. Stamm, A. Kiriy, *Macromolecules* **2010**, *43*, 77–81.

8 Note that the initiation rate constants (k_i) were obtained using the model system.

9 (a) R. Miyakoshi, K. Shimono, A. Yokoyama, T. Yokozawa, *J. Am. Chem. Soc.* **2006**, *128*, 16012–16013; (b) E. L. Lanni, A. J. McNeil, *J. Am. Chem. Soc.* **2009**, *131*, 16573–16579.

10 Excess iPrMgCl can terminate polymer chains via reacting with the catalyst during CTP. As a consequence, less than 1 equiv iPrMgCl is typically used.

11 B. E. Love, E. G. Jones. *J. Org. Chem.* **1999**, *64*, 3755–3756.

12 (a) A. D. Becke, *Phys. Rev. A* **1988**, *38*, 3098–3100; (b) J. P. Perdew, *Phys. Rev. B* **1986**, *33*, 8822–8824.

13 (a) R. Krishnan, J. S. Binkley, R. Seeger, J. A. Pople, *J. Chem. Phys.* **1980**, *72*, 650–654; (b) A. D. McLean, G. S. Chandler, *J. Chem. Phys.* **1980**, *72*, 5639–5648; (c) T. Clark, J. Chandrasekhar, G. W. Spitznagel, P. v. R. Schleyer, *J. Comp. Chem.* **1983**, *4*, 294–301.

14 (a) M. Dolg, U. Wedig, H. Stoll, H. Preuss, *J. Chem. Phys.* **1987**, *86*, 866–872; (b) J. M. L. Martin, A. Sundermann, *J. Chem. Phys.* **2001**, *114*, 3408–3420.

15 J. F. Hartwig, In Organotransition Metal Chemistry: From Bonding to Catalysis. University Science Books: Sausalito, CA, **2010**; pp. 321–345.

16 V. P. Ananikov, D. G. Musaev, K. Morokuma, *Organometallics.* **2005**, *24*, 715–723.

17 When the alkene was 2-butene, the crude reaction mixture contained the homodimerization product, consistent with disproportionation (SI).

18 Note that in the theoretical studies, X = Cl for all precatalysts (**2a**–**2f**). In the rate measurements, X = Cl for **2c**, **2e**, **2f** and X = Br for **2b** and **2d**.

19 Note that the initiation rate constant (k_i) cannot be obtained using equation 1 when it exceeds the propagation rate constant (k_p).

20 Note that the length of the alkyl chains has also changed, from methyl in the model system to hexyl in the polymerization.

21 In contrast, the propagation rate constant (k_p) was approx. 25% slower with Ph₃P present.

22 (a) A. M. Levine, R. A. Stockland, Jr, R. Clark, I. Guzei, *Organometallics* **2002**, *21*, 3278–3284; (b) R. Bertani, A. Berton, G. Carturan, R. Campostrini, *J. Organomet. Chem.* **1988**, *349*, 263–268; (c) R. J. McKinney, D. C. Roe, *J. Am. Chem. Soc.* **1986**, *108*, 5167–5173; (d) K. Tatsumi, A. Nakamura, S. Komiya, A. Yamamoto, T. Yamamoto, *J. Am. Chem. Soc.* **1984**, *106*, 8181–8188; (e) S. Komiya, Y. Abe, A. Yamamoto, T. Yamamoto, *Organometallics* **1983**, *2*, 1466–1468.

23 (a) T. Yamamoto, M. Abla, Y. Murakami, *Bull. Chem. Soc. Jpn.* **2002**, *75*, 1997–2009; (b) R. Giovannini, T. Studemann, A. Devasagayaraj, G. Dussin, P. Knochel, *J. Org. Chem.* **1999**, *64*, 3544–3553; (c) T. Yamamoto, M. Abla, *J. Organomet. Chem.* **1997**, *535*, 209–211.

24 (a) C.-Y. Huang, A. G. Doyle, *J. Am. Chem. Soc.* **2015**, *137*, 5638–5641; (b) C.-Y. Huang, A. G. Doyle, *J. Am. Chem. Soc.* **2012**, *134*, 9541–9544; (c) L. Estévez, L. W. Tuxworth, J.-M. Sotiropoulos, P. W. Dyer, K. Miqueu, *Dalton Trans.* **2014**, *43*, 11165–11179; (d) J. B. Johnson, T. Rovis, *Angew. Chem. Int. Ed.* **2008**, *47*, 840–871; (e) H. Kurosawa, H. Ohnishi, M. Emoto, N. Chatani, Y. Kawasaki, S. Murai, I. Ikeda, *Organometallics* **1990**, *9*, 3038–3042; (f) H. Kurosawa, H. Ohnishi, M. Emoto, Y.

Kawasaki, S. Murai, *J. Am. Chem. Soc.* **1988**, *110*, 6272–6273; (g) T. Yamamoto, A. Yamamoto, S. Ikeda, *J. Am. Chem. Soc.* **1971**, *93*, 3350–3359.

25 (a) H. A. Bronstein, C. K. Luscombe, *J. Am. Chem. Soc.* **2009**, *131*, 12894–12895; (b) S. D. Boyd, A. K.-Y. Jen, C. K. Luscombe, *Macromolecules* **2009**, *42*, 9387–9389.

26 Evans' pKa Table. http://evans.rc.fas.harvard.edu/pdf/evans_pKa_table.pdf (accessed December 6, **2016**).

27 The phrase refers to a quote by philosopher Ludwig Wittgenstein, who posited that "if a lion could talk, we would not understand him." For reference, see: L. Wittgenstein, Philosophical Investigations, 4th ed.; G. E. M. Anscombe, P. M. S. Hacker, J. Schulte, trans.; Blackwell Publishing Ltd: United Kingdom, **2009**; p. 327.

28 A common interpretation is that although we *would* be able to understand a talking lion, s/he would not be able to tell us about normal (non-talking) lions. S. Budiansky, If a Lion Could Talk: Animal Intelligence and the Evolution of Consciousness. Free Press; **1998**.

29 The percentages refer to the relative area ratios for each DP.

30 Similar ratios of end-groups were observed with precatalysts **2b–d** (SI).